

## Properties of Co-, Cr-, or Mn-implanted AlN

R. M. Frazier, J. Stapleton, G. T. Thaler, C. R. Abernathy, and S. J. Pearton<sup>a)</sup>

*Department of Materials Science and Engineering, University of Florida, Gainesville, Florida 32611*

R. Rairigh, J. Kelly, and A. F. Hebard

*Department of Physics, University of Florida, Gainesville, Florida 32611*

M. L. Nakarmi, K. B. Nam, J. Y. Lin, and H. X. Jiang

*Department of Physics, Kansas State University, Manhattan, Kansas 66506*

J. M. Zavada

*U.S. Army Research Office, Research Triangle Park, North Carolina 27709*

R. G. Wilson

*Consultant, Stevenson Ranch, California 91381*

(Received 17 March 2003; accepted 2 May 2003)

AlN layers grown on Al<sub>2</sub>O<sub>3</sub> substrates by metalorganic chemical vapor deposition were implanted with high doses ( $3 \times 10^{16} \text{ cm}^{-2}$ , 250 keV) of Co<sup>+</sup>, Cr<sup>+</sup>, or Mn<sup>+</sup>. Band-edge photoluminescence intensity at  $\sim 6 \text{ eV}$  was significantly reduced by the implant process and was not restored by 950 °C annealing. A peak was observed at 5.89 eV in all the implanted samples. Impurity transitions at 3.0 and 4.3 eV were observed both in implanted and unimplanted AlN. X-ray diffraction showed good crystal quality for the 950 °C annealed implanted samples, with no ferromagnetic second phases detected. The Cr- and Co-implanted AlN showed hysteresis present at 300 K from magnetometry measurements, while the Mn-implanted samples showed clear loops up to  $\sim 100 \text{ K}$ . The coercive field was  $< 250 \text{ Oe}$  in all cases. © 2003 American Institute of Physics. [DOI: 10.1063/1.1586987]

### INTRODUCTION

AlN plays an important role in many areas of solid-state devices, including thin film phosphors,<sup>1,2</sup> nitride-based metal-insulator-semiconductor heterostructure transistors,<sup>3,4</sup> thin-film gas sensors,<sup>5</sup> acoustic wave resonators,<sup>6,7</sup> ultraviolet light-emitting diodes,<sup>8–10</sup> distributed Bragg reflectors,<sup>11,12</sup> heat spreaders,<sup>13</sup> and heterojunction diodes.<sup>14</sup> AlN may also be promising in the emerging field of spintronics, due to its predicted high Curie temperature ( $T_C$ ) when doped with particular transition metals.<sup>15</sup> Room temperature ferromagnetism has been reported for Cr-doped AlN thin films deposited by reactive sputtering<sup>16</sup> or molecular beam epitaxy.<sup>17</sup> Ion implantation provides a versatile and convenient method for introducing transition metals into semiconductors for examination of their effects on the structural and magnetic properties of the resulting material.<sup>18</sup> AlN is an ideal host in this regard, since Kucheyev *et al.*<sup>19</sup> reported that single crystal epilayers of AlN grown on sapphire substrates did not become amorphous even at LN<sub>2</sub> temperatures for high doses of keV heavy ions such as Au. In addition, very high quality AlN on sapphire has recently been reported by several groups,<sup>20,21</sup> providing well-characterized material in which to examine the properties of transition metals.

In this article we report on the characteristics of Co-, Cr-, or Mn-implanted AlN. These appear to be the most promising elements for creation of robust ferromagnetism in AlN. In addition to the theory and experiments discussed

above for AlN,<sup>15,17</sup> room temperature ferromagnetism has been reported by several groups for Cr-doping of GaN.<sup>22–24</sup> The expected deep acceptor nature of the transition metals in AlN suggests that carrier-mediated ferromagnetism will be unlikely, but other mechanisms such as bound polarons may be applicable.<sup>25</sup>

### EXPERIMENT

The AlN epilayers were grown by metalorganic chemical vapor deposition on sapphire (0001) substrates, as described in detail elsewhere.<sup>20</sup> The layers were 1  $\mu\text{m}$  thick, with full-width-half-maximum values of 150–500 arc sec for the AlN (0002) rocking curves. Implantation of Cr<sup>+</sup>, Co<sup>+</sup>, or Mn<sup>+</sup> ions was carried out at an energy of 250 keV (corresponding to a projected range of  $\sim 1500 \text{ \AA}$  in each case) and a fixed dose of  $3 \times 10^{16} \text{ cm}^{-2}$ . The substrate temperature was held at  $\sim 300 \text{ °C}$  to promote dynamic annealing.<sup>26</sup> As a rough guide, the peak transition metal concentrations, located at the projected range, are  $\sim 3 \text{ at. \%}$  in the AlN. After implantation, the samples were annealed at 950 °C, 2 min under flowing N<sub>2</sub> in a Heatpulse 610T system. Photoluminescence (PL) measurements were carried out with a quadrupled Ti:sapphire laser as an excitation source together with a streak camera, providing an excitation power of  $\sim 3 \text{ mW}$  at 196 nm.<sup>27</sup> X-ray diffraction (XRD) was carried out on a Philips powder diffractometer while magnetic measurements were performed in a Quantum Design superconducting quantum interference device magnetic properties measurement system.

<sup>a)</sup> Author to whom correspondence should be addressed; electronic mail: spear@use.ufl.edu

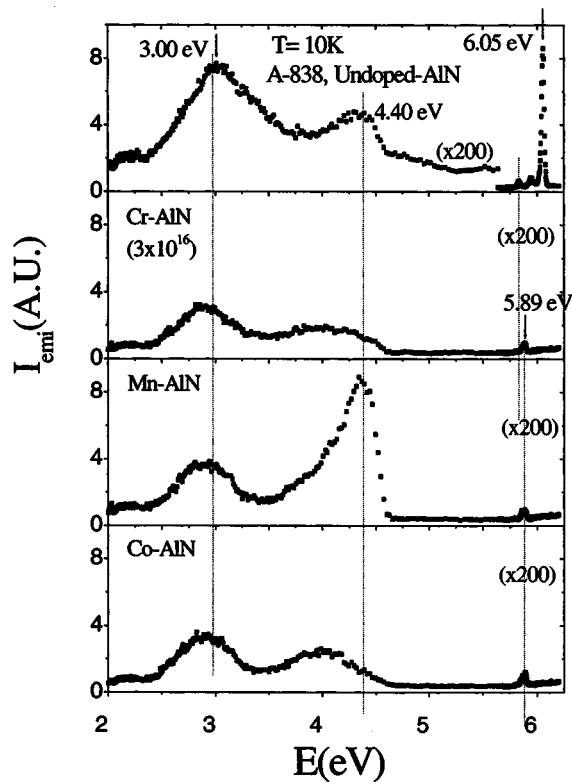


FIG. 1. 10 K PL spectra from AlN either before (top) or after  $\text{Cr}^+$ ,  $\text{Mn}^+$ , or  $\text{Co}^+$  implantation ( $3 \times 10^{16} \text{ cm}^{-2}$ , 250 keV), followed in all cases by 950 °C, 2 min anneals.

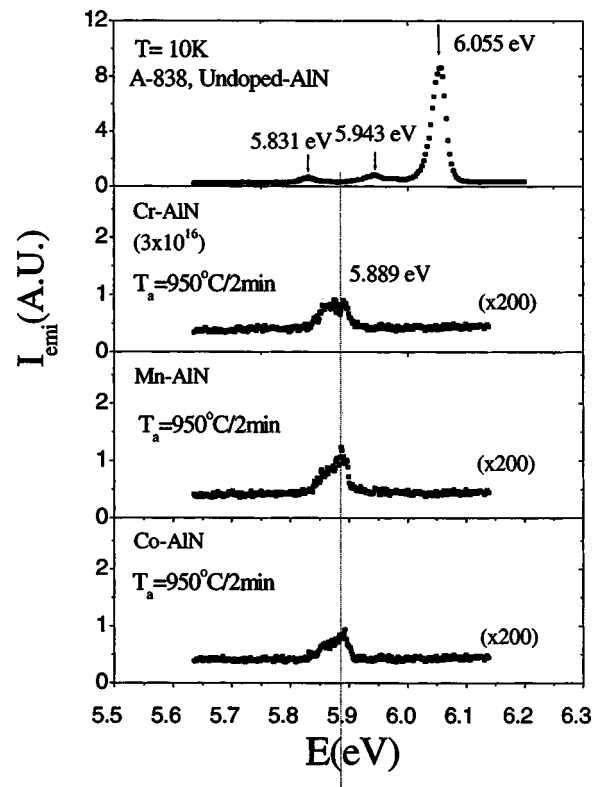


FIG. 2. 10 K AlN band edge region PL either before (top) or after  $\text{Cr}^+$ ,  $\text{Mn}^+$ , or  $\text{Co}^+$  implantation ( $3 \times 10^{16} \text{ cm}^{-2}$ , 250 keV), followed in all cases by 950 °C, 2 min anneals.

## RESULTS AND DISCUSSION

Figure 1 shows PL spectra taken at 10 K of the AlN implanted with Cr, Mn, or Co after annealing at 950 °C for 2 min. The spectra look basically identical in each case, even without annealing. The unimplanted AlN shows strong band-edge emission at  $\sim 6.05$  eV and two broad emission bands related with deep level impurities at  $\sim 3.0$  and 4.40 eV, each of which has peak intensity of  $\sim 1\%$  of the band-edge emission intensity. The Cr-, Mn-, and Co-implanted AlN show an absence of band-edge emission, which suggests that the point defect recombination centers created during implantation are stable against annealing at 950 °C. This is consistent with the conclusions of Kucheyev *et al.*,<sup>19</sup> who found that structural lattice disorder produced in AlN by 300 keV  $\text{Au}^+$  at doses comparable to those employed here was stable against rapid thermal annealing at 1000 °C.

Figure 2 shows an expanded view of the PL spectra in the band-edge region. Once again, the spectra were virtually unchanged as a result of the anneal at 950 °C. The transition lines at 5.943 and 5.831 eV are the one and two longitudinal optical (LO) phonon (112 meV) replica of the 6.055 eV emission line. The implanted samples all show a band at 5.889 eV, which is independent of the implanted species and most likely is related to lattice disorder induced by the implantation.

Figure 3 (top) shows a representative plot of magnetization versus field at 300 K for the Cr implanted AlN annealed at 900 °C. There is well-defined hysteresis present, with a coercive field of  $\sim 160$  Oe at 300 K and 230 Oe at 10 K. The

diamagnetic contributions from the substrate have been subtracted out of the data. At 300 K, the saturation moment,  $M_0 = g \mu_B S$ , where  $g$  is the degeneracy factor,  $\mu_B$  the Bohr magnetron, and  $S$  the total number of spins, was calculated to be  $\sim 0.65 \mu_B$  for Cr. This value is lower than the theoretical value of  $3 \mu_B$  expected for a half-filled  $d$  band of Cr, if all of the Cr ions were participating in the ferromagnetic signal. Disorder effects due to implantation-induced change may contribute to creating a distribution of exchange couplings that favor antiferromagnetism and reduce the effective magnetism. Plots of magnetization at 500 Oe versus temperature under field-cooled (FC) and zero-FC (ZFC) conditions are shown for the Cr-implanted AlN in the center of Fig. 3. This subtraction of FC and ZFC magnetization eliminates para- and diamagnetic contributions and indicates the presence of hysteresis if the difference is non-zero. The bottom of Fig. 3 shows the temperature dependence of this difference,  $\Delta M$ , with magnetization present to the 225–300 K range.

Similar data are shown in Fig. 4 for the Co-implanted AlN. Once again there is hysteresis present at 300 K, with a coercive field of  $\sim 1750$  Oe at 300 K and 240 Oe at 100 K and a calculated saturation moment of  $0.52 \mu_B$  for Co. The FC and ZFC magnetization versus temperature are shown at the bottom of the figure. In this case the differences extend to  $\sim 100$  K.

Figure 5 (top) shows magnetization versus field at 100 K for Mn-implanted AlN. This was the highest temperature for which clear hysteresis could be obtained. The coercive field

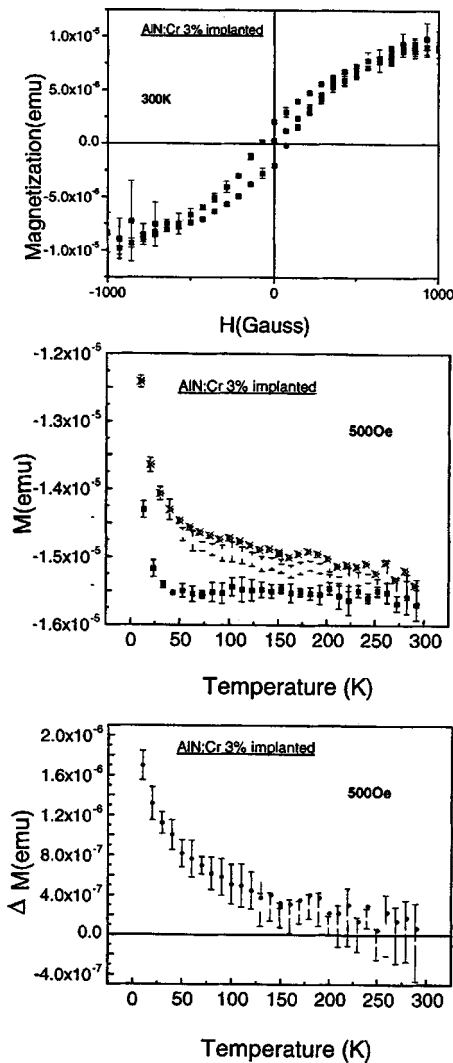


FIG. 3. 300 K magnetization as a function of field (top), field-cooled (FC), and zero-field-cooled (ZFC) magnetization vs temperature (center) and difference in FC-ZFC magnetization vs temperature for AlN implanted with  $3 \times 10^{16} \text{ cm}^{-2} \text{ Cr}^+$  and annealed at  $950^\circ \text{C}$ , 2 min.

was  $\sim 220$  Oe at both 100 and 10 K. The FC and ZFC phases are almost coincident at an applied field of 500 Oe, as shown at the bottom of the figure and consistent with lower overall magnitude of the magnetization. The calculated saturation moment was  $0.17 \mu_B$  for Mn at 100 K, compared to the theoretical value of 4.

Figure 6 shows representative  $\theta$ - $2\theta$  XRD scans of the Cr or Mn implanted samples after  $950^\circ \text{C}$  annealing. The Co data are not shown for clarity sake, since the spectra was the same as for the Mn and Cr implanted material. The main peaks correspond to the expected AlN(0002) and (0004) lines and  $\text{Al}_2\text{O}_3$  (0002), (0006), and (0012) substrate peaks and the broad peak at  $2\theta = 20^\circ$  is due to short-range disorder from the implantation process and was not observed on the as-grown films. No peaks due to the half-metallic ferromagnetic  $\text{CrO}_2$  phase<sup>28</sup> were detected in the Cr-implanted sample and other potential second phases which could form, such as Cr,  $\text{CrN}$ ,<sup>29</sup>  $\text{Cr}_2\text{N}$  and  $\text{Al}_x\text{Cr}_y$ , were not detected and in any case are not ferromagnetic at the temperatures used in

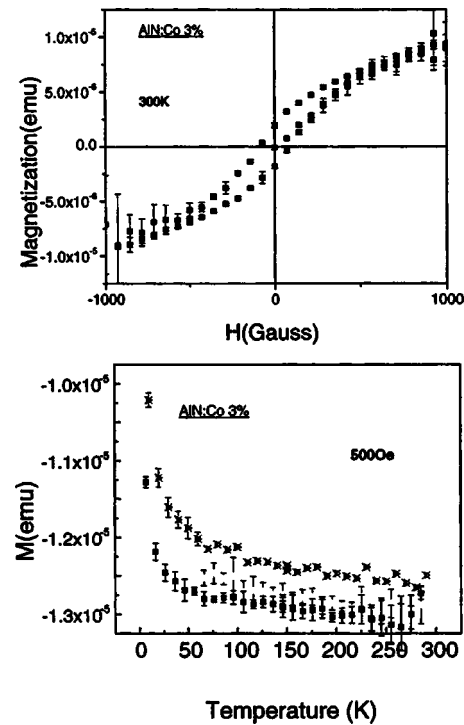


FIG. 4. 300 K magnetization as a function of field (top) and FC and ZFC magnetization as a function of temperature (bottom) for AlN implanted with  $3 \times 10^{16} \text{ cm}^{-2} \text{ Co}^+$  and annealed at  $950^\circ \text{C}$ , 2 min.

these experiments.<sup>24</sup> Similarly, in the case of Co implantation, metallic Co has a Curie temperature of 1382 K and  $\text{Co}_x\text{N}$  phases are all Pauli ferromagnetic.<sup>30</sup> Finally, for Mn implantation, metallic Mn is antiferromagnetic<sup>24</sup> while  $\text{Mn}_x\text{N}$

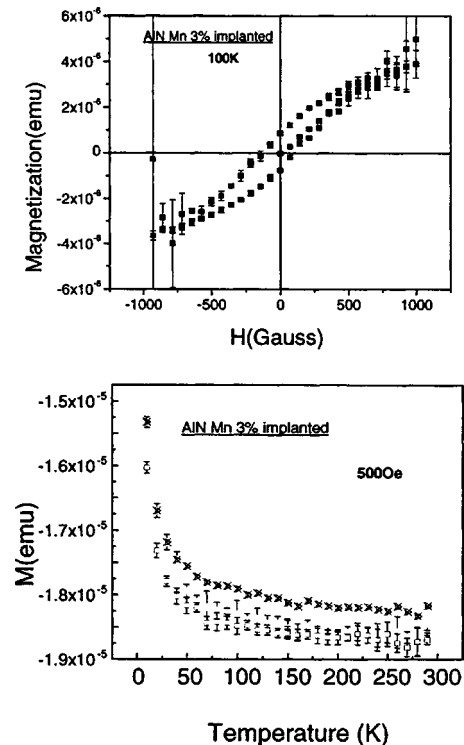


FIG. 5. 100 K magnetization as a function of field (top) and FC and ZFC magnetization as a function of temperature (bottom) for AlN implanted with  $3 \times 10^{16} \text{ cm}^{-2} \text{ Mn}^+$  and annealed at  $950^\circ \text{C}$ , 2 min.

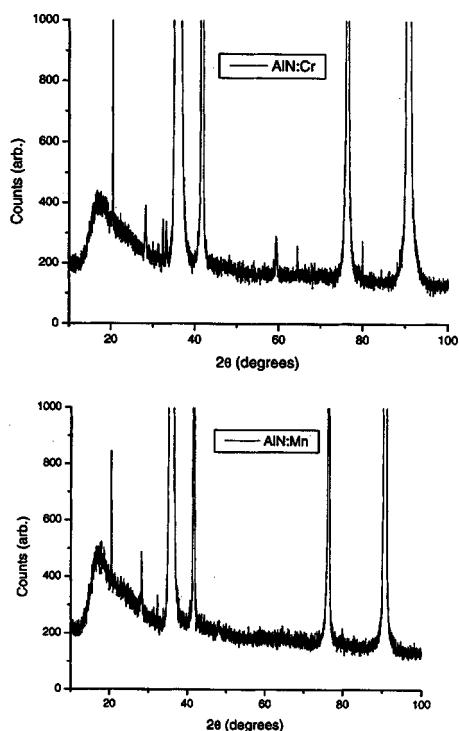


FIG. 6. X-ray diffraction scans of AlN implanted with  $\text{Cr}^+$  (top) or  $\text{Mn}^+$  (bottom) to a dose of  $3 \times 10^{16} \text{ cm}^{-2}$  and annealed at  $950^\circ\text{C}$ , 2 min.

is ferromagnetic with a Curie temperature of 745 K.<sup>24</sup> Thus, secondary ferromagnetic phases are not responsible for the observed magnetic properties.

The origin of the observed ferromagnetism is not likely to be carrier-mediated due to the insulating nature of the AlN. Wu *et al.*<sup>17</sup> suggested that substitutional  $\text{Al}_x\text{Cr}_{1-x}\text{N}$  random alloys would have Curie temperatures over 600 K, as estimated from a multicomponent mean-field theory in which the ferromagnetism occurs in a midgap defect band. Another possible mechanism for the observed magnetic properties is that the Mn is not randomly distributed on Al sites but is present as atomic scale clusters. Some mean field theories suggest that Mn clustering can significantly influence  $T_c$  as a result of the localization of spin polarized holes near regions of higher Mn concentration.<sup>31,32</sup> There is also some support for this assertion from local spin density approximation calculations which predict it is energetically favorable for the formation of magnetic ion dimers and trimers at second nearest-neighbor sites which are ferromagnetic.<sup>32</sup> The percolation network-like model for ferromagnetism in low carrier concentration systems suggested by several groups is another potential mechanism.<sup>33,34</sup>

## SUMMARY AND CONCLUSIONS

High doses ( $3 \times 10^{16} \text{ cm}^{-2}$ ) of ion implanted  $\text{Co}^+$ ,  $\text{Cr}^+$ , or  $\text{Mn}^+$  ions into AlN epilayers on  $\text{Al}_2\text{O}_3$  substrates severely degrades the band-edge luminescence, which is not recovered by annealing up to  $950^\circ\text{C}$ . In each case the implanted AlN shows ferromagnetic ordering as evidenced by the presence of hysteresis in  $M$  versus  $H$  loops. The hysteresis persists up to  $\geq 300$  K in the case of  $\text{Cr}^+$  or  $\text{Co}^+$  implantation and 100 K for  $\text{Mn}^+$  implantation. Less than  $\sim 20\%$  of the

implanted ions contribute to the magnetization, but this might be increased by use of much higher annealing temperatures. Simple two-terminal resistivity measurements show that the implanted AlN remains insulating ( $>10^8 \Omega \text{ cm}$ ) and thus conventional carrier-mediated ferromagnetism is not a likely mechanism for the observed magnetic properties. Implantation provides a versatile method of introducing different transition metal dopants into AlN for examination of their effect on the structural and magnetic properties.

## ACKNOWLEDGMENTS

The work at UF was partially supported by Grant Nos. NSF DMR0101438 and ECS 02242203 and by ARO under Grant Nos. DAAF 190110701 and 19021420. The work at K.S.U. was partially supported by ARO and NSF (Grant No. DMR-9902431).

- <sup>1</sup>A. L. Martin, C. M. Spalding, E. I. Dimitrova, P. G. Van Patten, M. C. Caldwell, M. E. Kordesch and H. H. Richardson, *J. Vac. Sci. Technol. A* **19**, 1894 (2001).
- <sup>2</sup>F. Lu, R. Carius, A. Alam, M. Heuken, and Ch. Buchal, *J. Appl. Phys.* **92**, 2457 (2002).
- <sup>3</sup>D.-H. Cho, M. Shimizu, T. Ide, H. Ookita, and H. Koumwa, *Jpn. J. Appl. Phys., Part 1* **41**, 4481 (2002).
- <sup>4</sup>X. Hu *et al.*, *Appl. Phys. Lett.* **82**, 1299 (2003).
- <sup>5</sup>F. Serina, K. Y. S. Ng, C. Huang, G. W. Amer, L. Romni, and R. Naik, *Appl. Phys. Lett.* **79**, 3350 (2001).
- <sup>6</sup>S.-H. Lee, J.-K. Lee, and K. H. Yoon, *J. Vac. Sci. Technol. A* **21**, 1 (2003).
- <sup>7</sup>Y. Takagaki, P. Santos, E. Wiebicke, O. Brandt, J. D. Schmerr, and K. Ploog, *Appl. Phys. Lett.* **81**, 2538 (2002).
- <sup>8</sup>G. Kipshidze, V. Kuryatkov, K. Zhu, B. Vorizov, M. Holtz, S. Nikishin, and H. Temkin, *J. Appl. Phys.* **93**, 1363 (2003).
- <sup>9</sup>T. Nishida, N. Kobayashi, and T. Ban, *Appl. Phys. Lett.* **82**, 1 (2003).
- <sup>10</sup>R. Gaska *et al.*, *Appl. Phys. Lett.* **81**, 4658 (2002).
- <sup>11</sup>K. E. Waldrip, J. Han, J. J. Figel, H. Zhou, E. Maharama, and A. V. Normikko, *Appl. Phys. Lett.* **78**, 3205 (2001).
- <sup>12</sup>A. Bhattacharya, S. Iyer, E. Iliopoulos, A. V. Samparth, J. Cabalu, T. D. Moustakas, and I. Friel, *J. Vac. Sci. Technol. B* **20**, 1229 (2002).
- <sup>13</sup>S. N. Yoganand, K. Jaqannadhan, A. Karoui, and H. Wang, *J. Vac. Sci. Technol. A* **20**, 1974 (2002).
- <sup>14</sup>C. R. Miskys, J. A. Garrido, C. Nebel, M. Hermann, O. Ambacher, M. Eickhoff, and M. Stutzmann, *Appl. Phys. Lett.* **82**, 290 (2003).
- <sup>15</sup>V. I. Litvinov and V. K. Dugaev, *Phys. Rev. Lett.* **86**, 5593 (2001).
- <sup>16</sup>S. G. Yang, A. B. Pakhomov, S. T. Hung, and C. Y. Wong, *Appl. Phys. Lett.* **81**, 2418 (2002).
- <sup>17</sup>S. Y. Wu, H. X. Liu, L. Gu, R. K. Singh, L. Budd, M. Schilfgaarde, M. R. McCartney, D. J. Smith, and N. Newman, *Appl. Phys. Lett.* **82**, 3047 (2003).
- <sup>18</sup>N. Theodoropoulou, A. F. Hebard, M. E. Overberg, C. R. Abernathy, S. J. Pearton, S. N. G. Chu, and R. G. Wilson, *Phys. Rev. Lett.* **89**, 107203 (2003).
- <sup>19</sup>S. O. Kucheyev, J. S. Williams, J. Zou, C. Jaegadish, M. Pophristic, S. Guo, I. T. Ferguson, and M. O. Manasreh, *J. Appl. Phys.* **92**, 3554 (2002).
- <sup>20</sup>J. Li, K. B. Nam, M. C. Nakarmi, J. Y. Lin, and H. X. Jiang, *Appl. Phys. Lett.* **81**, 3365 (2002).
- <sup>21</sup>E. Kuokstis *et al.*, *Appl. Phys. Lett.* **81**, 2755 (2002).
- <sup>22</sup>M. Hastimoto, Y.-K. Zhou, M. Kanamura, and H. Asahi, *Solid State Commun.* **122**, 37 (2002).
- <sup>23</sup>S. E. Park, H.-J. Lee, Y. C. Cho, S.-Y. Jeong, C. R. Cho, and S. Cho, *Appl. Phys. Lett.* **80**, 4187 (2002).
- <sup>24</sup>S. J. Pearton, C. R. Abernathy, D. P. Norton, A. F. Hebard, Y. D. Park, L. A. Boatner, and J. D. Budai, *Mater. Sci. Eng., R.* **40**, 137 (2003).
- <sup>25</sup>T. Gral, M. Gjukic, M. S. Brandt, M. Stutzmann, and O. Ambacher, *Appl. Phys. Lett.* **81**, 5159 (2002).
- <sup>26</sup>J. S. Williams, *Mater. Sci. Eng., A* **253**, 9 (1998).
- <sup>27</sup>K. B. Nam, J. Li, K. H. Kim, J. Y. Lin, and H. X. Jiang, *Appl. Phys. Lett.* **78**, 3690 (2001).
- <sup>28</sup>Y. Ji, G. J. Stijfers, F. Y. Yang, C. C. Chien, J. M. Byers, A. Angelovch, G. Xiao, and A. Gupta, *Phys. Rev. Lett.* **86**, 5585 (2001).

- <sup>29</sup>K. Inumarn, H. Okamoto, and S. J. Yamanka, *J. Cryst. Growth* **237–239**, 2050 (2002).
- <sup>30</sup>K. Suzuki, T. Kancho, H. Yoshida, H. Morita, and H. Fujimori, *J. Alloys Compd.* **224**, 232 (1995).

- <sup>31</sup>A. L. Chudnovskiy and D. Pfannkuche, *Phys. Rev. B* **65**, 165216 (2002).
- <sup>32</sup>M. van Schilfgaarde and O. N. Mryasov, *Phys. Rev. B* **63**, 233205 (2001).
- <sup>33</sup>M. Bercui and R. N. Bhatt, *Phys. Rev. Lett.* **87**, 107203 (2001).
- <sup>34</sup>A. Kaminski and S. D. Sarma, *Phys. Rev. Lett.* **88**, 247202 (2002).